Preserving Inter-Brain Coupling: A Constraint-based Preprocessing Method for Collaborative Multi-brain Motor Imagery

Li Zhu (zhuli@hdu.edu.cn)[1,2], Xinlei Chen (252050193@hdu.edu.cn)[1], Mengqi Tu (251050015@hdu.edu.cn)[1], Yunqi Shi (yunqi@hdu.edu.cn)[1], Andrzej Cichocki (cichockiand@gmail.com)[3] & Wanzeng Kong (kongwanzeng@hdu.edu.cn)[1,2]

[1]School of Computer Science and Technology, Hangzhou Dianzi University, Hangzhou, Zhejiang, China

[2]Zhejiang Provincial Key Laboratory of Brain Computer Collaborative Intelligence Technology and Applications, Hangzhou Dianzi University, Hangzhou, Zhejiang, China

[3]Laboratory of Intelligent Systems, Systems Research Institute, Warsaw, Poland

Abstract

Traditional collaborative Brain Computer Interface (cBCI) pipelines treat participants as independent entities, inadvertently suppressing inter-brain neural dependencies critical for hyperscanning-based tasks. We propose an Inter-brain Coupling-Constrained Independent Component Analysis (ICC-ICA) method that incorporates a coupling gradient into the objective function to preserve shared neural signatures. Validated on a motor imagery (MI) dataset, our approach demonstrates that integrating inter-brain constraints does not compromise signal quality, yielding a stable 1.76% accuracy improvement. Crucially, functional network analysis reveals enhanced recovery of inter-brain links primarily localized in task-relevant motor regions. Furthermore, ICC-ICA shows superior retention of both intra-frequency and cross-frequency coupling across the entire task duration. These findings demonstrate that explicitly regularizing the ICA update rule with inter-participant constraints effectively safeguards social brain markers, providing a robust foundation for group-level neural decoding and more valid collaborative BCI systems.

Keywords: Collaborative brain computer interface; Inter-brain coupling; Independent component analysis; Functional network; Motor imagery

Introduction

In the past decade, Brain-Computer Interfaces have transitioned from individual-centric to collaborative paradigms (cBCIs) (Salvatore et al., 2022), utilizing hyperscanning to explore social coordination (Carollo and Esposito, 2024; Speer et al., 2024). However, raw Electroencephalogram(EEG) is a complex convolved signal where clean neural activity is deeply masked by intense artifacts. To extract reliable neural representations, a variety of preprocessing techniques have been widely adopted, including filtering, Canonical Correlation Analysis (CCA) (Cherloo et al., 2022), Wavelet Transform (WT) (Yan et al., 2023), Empirical Mode Decomposition (EMD) (Yao et al., 2023), and hybrid methods (Liu et al., 2021). Among these, Independent Component Analysis (ICA) (Buchholz et al., 2022; Gao et al., 2022) remains the most prevalent gold standard. Critically, despite their algorithmic differences, these methods share a common theoretical premise: they all rely on the statistical independence or morphological separability between effective neural components and artifacts to achieve denoising.

In standard cBCI pipelines, preprocessing is customarily applied to each participant individually, antecedent to any collaborative modeling (Czeszumski et al., 2020). However, this isolated optimization strategy introduces a fundamental theoretical paradox. By strictly enforcing statistical independence within a single brain to distinguish signals from noise (Hyvärinen and Oja, 2000), these algorithms inherently disregard the inter-brain coupling structure. Consequently, the synchronized neural dynamics which are the essence of social interaction are prone to being misinterpreted as redundant artifacts or mathematically orthogonalized during this unconstrained separation process.

To resolve this conflict between intra-participant independence and inter-participant coupling, we propose the Inter-brain Coupling-Constrained Independent Component Analysis (ICC-ICA) algorithm. Unlike traditional methods, ICC-ICA integrates an inter-participant coupling gradient into the ICA optimization framework, ensuring that the separation of independent components is regularized by the inter-brain synchrony. Furthermore, we developed an automated component judgment module based on kurtosis and spatial priors to ensure efficient and objective artifact rejection.

Our experimental results demonstrate that ICC-ICA significantly outperforms state-of-the-art (SOTA) models in both decoding accuracy and the preservation of functional connectivity. Through comprehensive analysis, we identified that $(\alpha-\beta)$ cross-frequency coupling serves as a primary bridge for inter-brain synchronization during collaborative MI tasks. Beyond more performance gains, the proposed framework offers a theoretically grounded solution to the intrinsic dilemma between intra-brain independece and inter-brain coupling. The main contributions of this study are summarized as follows:

- We develop a novel coupling-constrained ICA framework (ICC-ICA) specifically architected for hyperscanning scenarios, effectively balancing individual signal purity with inter-brain dependency;
- We provide empirical evidence that integrating inter-brain constraints enhances the decoding of collaborative intentions;
- Our findings elucidate the frequency-dependent and temporal dynamics of inter-brain hyper-connectivity during motor imagery, providing a deeper understanding of the neural underpinnings of social coordination.

In G. Boleda, I. Dautriche, M. Maldonado, C. Saldana and T. Torrent (Eds.), *Proceedings of the 48th Annual Conference of the Cognitive Science Society*

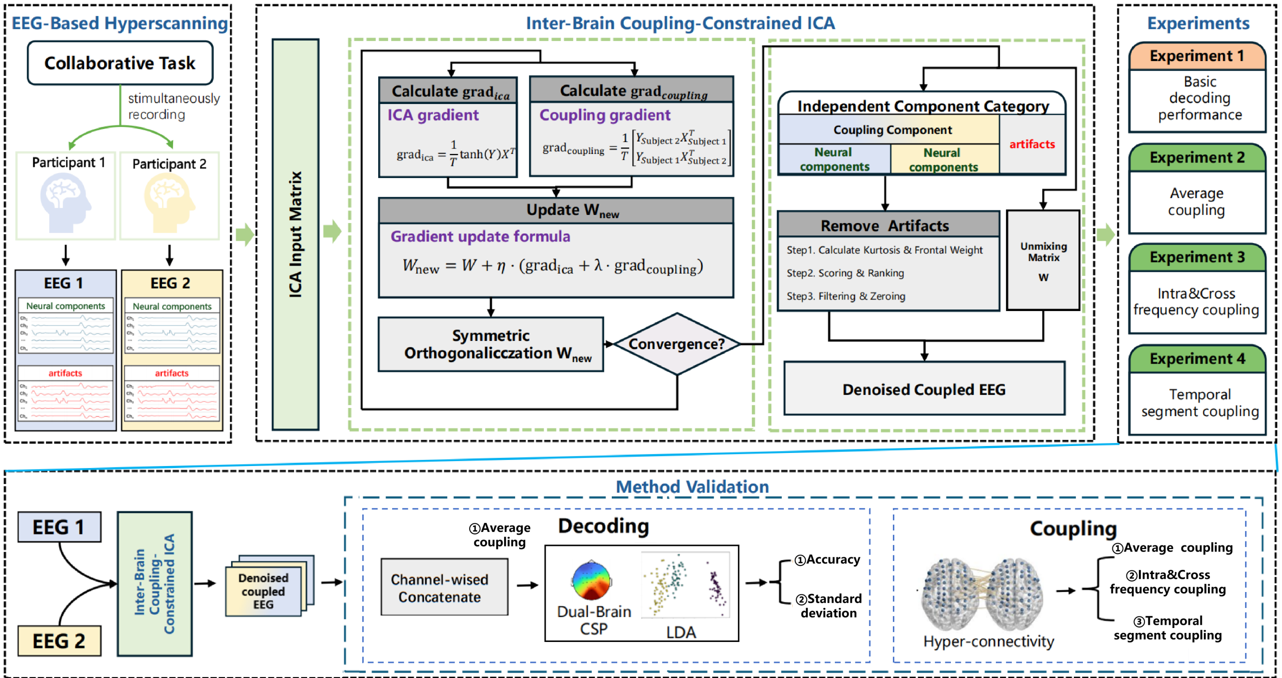

Figure 1: The architecture of the proposed ICC-ICA framework. The pipeline consists of three main stages: EEG-based hyperscanning input from collaborative tasks; The Inter-Brain Coupling-Constrained ICA module, which updates the weight matrix W by integrating both the ICA gradient and the coupling gradient to preserve inter-participant phase-locking while removing artifacts; Method validation involving MI classification decoding and hyperconnectivity analysis.

Related Works

Hyperscanning-based social interaction and collaborative multi-brain brain computer interface

Social interaction requires mutual neural adjustment between individuals. Hyperscanning uses hyper-connectivity metrics, like phase synchronization, to characterize inter-brain coupling during collaborative tasks. Specifically, synchrony in motor and parietal regions facilitates temporal coordination, while link strength reflects trust and consensus in joint decision-making.

Building on this, cBCI have shifted from individual to group-enhanced systems. By leveraging shared neural signatures, cBCIs integrate multi-brain data to improve decoding robustness. Here, inter-brain coupling serves as a vital informational bridge for optimizing group performance. Consequently, preserving these coupling signatures during signal processing is essential for advancing high-performance hyperscanning applications.

Pre-processing method for EEG-based hyperscanning scenarios

Reliable EEG analysis requires effective pre-processing to eliminate artifacts like Electrooculogram and Electromyography (Almutairi et al., 2023; Sharma et al., 2022). Traditionally, ICA has been the cornerstone of single-brain denoising due to its ability to isolate non-neural sources. However, as research shifts toward hyperscanning, the limitations of these individual-centric methods have surfaced.

Currently, the prevailing approach denoises each participant separately before analyzing inter-brain dependencies. This sequential strategy often overlooks the intrinsic correlations between participants. Because standard ICA maximizes individual non-Gaussianity, it may inadvertently suppress or distort synchronized inter-brain signatures by treating them as noise. Consequently, an integrated framework is required to process dual-brain data simultaneously, ensuring that artifacts are removed without compromising essential inter-brain links.

Motor imagery mechanism and decoding

MI involves the mental rehearsal of movement, sharing neural substrates with motor execution. Its primary neurophysiological hallmarks are Event-Related Desynchronization (ERD)(Byrne et al., 2025; Pronina et al., 2023) and Synchronization (ERS) (Bardel et al., 2024; Marques et al., 2022) within the α (8–13 Hz) and β (13–30 Hz) rhythms. Traditionally, decoding these patterns relies on the Common Spatial Pattern (CSP)(Apicella et al., 2022; Lin et al., 2023) to maximize variance between classes, often coupled with Linear Discriminant Analysis(LDA)(Zhao et al., 2024) or Support Vector Machine for robust intention identification.

However, cBCI adds complexity by requiring the integration of individual intentions with shared goals. While cBCI leverages complementary information between participants to improve accuracy, performance remains highly sensitive to signal-to-noise ratios and rhythmic integrity. Since joint tasks induce subtle inter-brain synchronization, any distortion of oscillatory components during pre-processing can degrade classification accuracy. Consequently, effective cBCI decoding demands high-fidelity signals that preserve both individual ERD/ERS patterns and inter-participant coordination signatures.

Methods

The architecture of the proposed ICC-ICA framework is illustrated in Figure 1. The framework integrates a coupling constraint module into the decomposition process. After synchronizing EEG signals and applying filtering, the algorithm explicitly preserves inter-participant phase-locking information during the weight matrix update. Finally, reconstructed signals are used for hyperconnectivity analysis and MI classification, ensuring that critical social brain markers are preserved.

Dual-brain hyperscanning EEG motor imagery recording

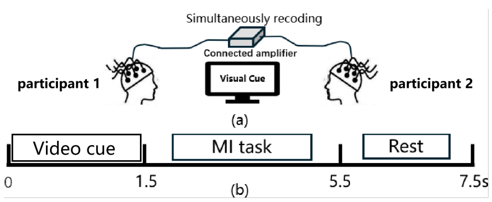

Figure 2: Experimental setup and procedure. (a) Dual-participant EEG hyperscanning setup for capturing inter-brain dynamics. (b) The temporal structure of a single trial.

A synchronized dual-brain hyperscanning system was established using two Neuroscan SynAmps2/RT amplifiers (Figure 2a). EEG data were recorded via 62-channel Ag/AgCl caps (10-20 System) at 1000 Hz with impedance < 5 kΩ. The paradigm (Figure 2b) comprised a 1.5s cue, 4s motor imagery task, and 3s rest. In total, 375 trials were acquired for each participant pair. Twenty-two participants (11 pairs) provided written informed consent to participate.

Inter-brain coupling-constrained independent component analysis

independent component analysis ICA is a blind source separation algorithm primarily used to separate multiple signals from a mixed signal. Its underlying assumption is that the source signals belong to non-Gaussian distributions and are statistically independent of each other. In EEG processing, the observed scalp signal $X \in \mathbb{R}^{N\times T}$ is considered, where N represents the number of electrodes and T denotes the number of recorded time points. The decomposition model for the established hidden independent sources S is as follows:

$$X = AS \tag{1}$$

Where A represents the mixing matrix. The goal of ICA is to find a demixing matrix W such that the estimated source signals $Y = WX$ are statistically as independent as possible, which is usually achieved by maximizing the non-Gaussianity of the components or minimizing the mutual information between components.

However, in traditional cBCI research, ICA is typically calculated independently for each participant. Although this traditional method can effectively remove eye movement and electromyographic artifacts from participants, it ignores the neural dependencies across participants' brains. By treating each participant as an isolated entity, standard ICA may inadvertently suppress or distort the synchronous neural features that are crucial for understanding social coordination and joint task performance in the hyperscanning paradigm.

Inter-brain coupling-constrained module To bridge the gap in inter-brain dependency preservation, we propose a coupling-constrained optimization rule. The core innovation lies in the modification of the gradient descent process by integrating a coupling gradient, $grad_{coupling}$, into the traditional ICA update framework.

Specifically, the ICA gradient, $grad_{ica}$, which ensures the statistical independence of components within a single participant, is defined as:

$$grad_{ica} = \frac{1}{T} tanh(Y)X^T \tag{2}$$

where Y represents the estimated independent components and X is the observed EEG data. To explicitly safeguard the neural synchrony between participant pairs, we define the inter-brain coupling gradient as:

$$grad_{coupling} = \frac{1}{T}\begin{bmatrix} Y_{participant2}X^T_{participant1} \\ Y_{participant1}X^T_{participant2} \end{bmatrix} \tag{3}$$

This term captures the cross-participant interaction by projecting the neural activity of one participant onto the observation space of the other. The final update rule for the unmixing matrix W is formulated as:

$$W_{new} = W + \eta \cdot (grad_{ica} + \lambda \cdot grad_{coupling}) \tag{4}$$

where η denotes the learning rate and λ is a regularization parameter that controls the trade-off between intra-brain independence and inter-brain coupling. By incorporating this constraint, the ICC-ICA algorithm is forced to converge toward a solution that not only identifies clean neural sources but also prioritizes the retention of shared rhythmic signatures across the two brains.

Automatic components judgment module To ensure the standardization and efficiency of the denoising process, we have implemented an automatic component identification module that identifies and eliminates artifacts through a systematic three-step process. Firstly, the module calculates the kurtosis and Frontal Weight of each extracted IC, aiming to assess its statistical distribution characteristics and spatial origin, particularly targeting high-peak myoelectric activity and ocular movement artifacts concentrated in the frontal lobe region. Subsequently, a comprehensive scoring and ranking mechanism is applied to prioritize each independent component based on these quantitative indicators, thereby distinguishing between effective neural signals and non-EEG artifacts. Finally, in the filtering and zeroing stage, components exceeding a preset empirical threshold are systematically removed, their corresponding rows in the demixing matrix are cleared to zero, and the cleaned EEG data are reconstructed by back-projecting to the electrode space, thus achieving denoising while retaining core inter-brain coupling features.

Model setup and verfication

Model parameters and operating environment configuration ICC-ICA and the validation pipeline were implemented in Python 3.12, leveraging MNE-Python (v1.11) for EEG manipulation, Scipy (v1.17) for signal processing, and NumPy for matrix operations.

During optimization, the unmixing matrix W was initialized via Gaussian distribution and QR decomposition. We set the learning rate $\eta = 0.01$ and the coupling parameter $\lambda = 0.2$ to balance independence and synchrony. Convergence was defined at 1×10^{-9} (max 200 iterations), with symmetric orthogonalization applied each step to prevent component collapse. For artifact rejection, a kurtosis threshold of 5.0 and a frontal-electrode spatial prior were utilized. All computations were performed on an AMD Ryzen 9 9950X workstation with 64GB RAM to ensure efficient processing.

Experiments on inter-brain coupling preserving Common spatial potential and extension for collaborative motor imagery To evaluate the efficacy of ICC-ICA in preserving task-relevant features, we employed the CSP algorithm and LDA classifier as benchmarks. In our collaborative MI context, the standard CSP was extended to handle the concatenated dual-brain signal space and multi-class tasks. For the three-class problem, we adopted a one-vs-rest (OVR) strategy. For each class i, the spatial filter W_i is obtained by solving the generalized eigenvalue problem:

$$\Sigma_i W_i = \lambda(\Sigma_i + \bar{\Sigma}_i) W_i \tag{5}$$

where Σ_i is the average covariance matrix of class i, and $\bar{\Sigma}_i$ is the sum of the covariance matrices of the remaining classes. The feature vector f for each trial is constructed by projecting the joint spatial-temporal matrix E using the optimized filters: $Z = W_{csp}E$, where $f = \log(\mathrm{var}(Z))$.Subsequently, the LDA classifier determines the task category by finding a projection vector w that maximizes the ratio of between-class variance to within-class variance. For multi-class classification, the decision function $g(x)$ assigns the input to the class with the highest posterior probability. By analyzing the resulting accuracy, we quantified the impact of inter-brain coupling on the discriminability of μ and β rhythms.

Phase locked value connectivity and extension for collaborative motor imagery To quantitatively assess the degree of preservation of inter-participant neural dependency, we calculated the trial-averaged Phase Locking Value (PLV) matrices for all participants across different task categories. PLV is a widely used metric to quantify the phase synchronization between two neural signals in a specific frequency band, independent of their power or amplitude. For two EEG signals $x_i(t)$ and $x_j(t)$, the PLV is defined as:

$$PLV = \frac{1}{T} \left| \sum_{t=1}^{T} e^{j(\phi_i(t) - \phi_j(t))} \right| \tag{6}$$

where T denotes the number of time points, and $\phi_i(t)$ and $\phi_j(t)$ represent the instantaneous phases of the signals at time t, typically obtained via the Hilbert transform.

To isolate genuine neural coupling from noise, we performed significance testing on PLV values, specifically focusing on motor-related regions. The count of electrode pairs exceeding the significance threshold ($p < 0.05$) served as the primary quantitative metric. By comparing the volume of significant hyper-links between standard ICA and ICC-ICA, we evaluated the algorithm's efficacy in preserving social brain markers. A higher retention of connections in the ICC-ICA condition would verify that the coupling constraint effectively prevents the unintentional suppression of inter-participant synchrony during component decomposition.

Experiments and Results

Comparisons on decoding performance with SOTA model

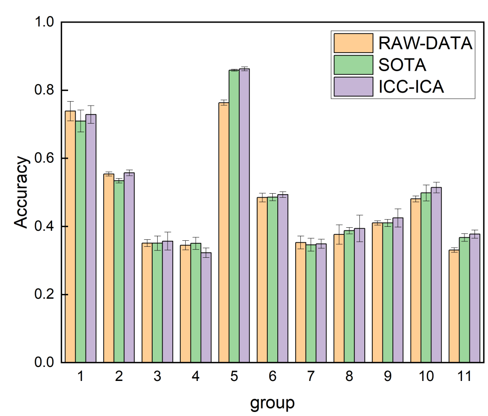

Figure 3: Classification accuracy across groups. Performance is compared among raw data, SOTA, and ICC-ICA methods. Error bars represent standard errors.

In this section, we evaluate the decoding performance of our proposed ICC-ICA method against the existing SOTA processes and benchmark models. The benchmark model directly processes the raw data using traditional CSP combined with LDA. The SOTA process consists of standard ICA denoising and the same CSP/LDA classifier. As shown in

Figure 3, which compares the classification accuracy of each group, our ICC-ICA method outperforms SOTA in both average performance and across most groups. Specifically, the data processed by ICC-ICA achieves a 1.76% improvement in decoding accuracy compared to the benchmark CSP/LDA, and a 0.8% improvement compared to the SOTA standard ICA process. These results indicate that, while traditional ICA only focuses on individual independent components, by introducing inter-brain coupling constraints, it can effectively preserve more discriminative neural information, thereby achieving more robust decoding in collaborative motor imagery tasks.

Inter-brain coupling analysis using PLV-based hyperconnectivity

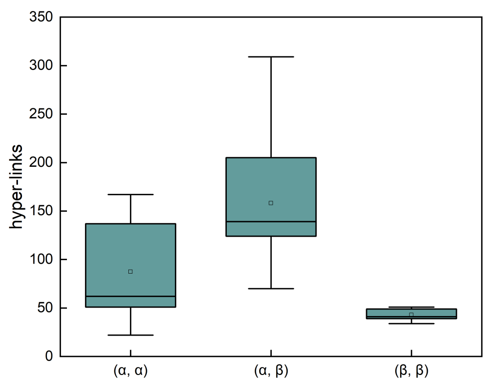

Figure 4: Distribution of significant hyper-connectivity links across intra- and cross-frequency bands.

To investigate the impact of the coupled constraint module on interbrain neural dependency, we conducted a comparative hyperconnectivity analysis using PLV. As shown in Figure 5, we counted the number of hyperconnectivity pairs that passed the significance test ($p < 0.05$) within the motor-related regions across all groups. The experimental results indicated that, compared to the group without using ICC-ICA constraints, the data processed by ICC-ICA exhibited significantly higher numbers of hyperconnectivity pairs in all participant pairs. This enhancement was particularly concentrated in task-related motor areas (such as C3, Cz, and C4), suggesting that traditional ICA, while pursuing individual component independence, inadvertently filters out cross-brain synchronous neural oscillations. By explicitly incorporating inter-participant constraints in the update rule, ICC-ICA effectively preserves these critical social brain markers, providing a more robust physiological foundation for understanding interbrain coordination during collaborative motor imagery.

Table 1: Decoding accuracy for 11 groups under three frequency settings. Bold numbers denote the best performance for each group.

Group	(α, α)	$(\alpha \Longleftrightarrow \beta)$	(β, β)
1	32.80±2.17	37.60±5.88	**65.60±7.56**
2	30.40±6.44	32.80±6.95	**43.47±5.17**
3	35.20±3.11	**39.47±3.53**	37.60±6.50
4	34.40±4.17	**35.87±4.16**	35.47±5.17
5	38.67±4.22	44.94±4.91	**84.80±4.81**
6	29.07±5.56	34.94±3.66	**44.80±2.61**
7	32.00±3.96	34.00±4.90	**38.13±2.75**
8	35.20±7.19	37.73±6.32	**38.40±9.63**
9	35.47±5.63	35.87±7.52	**42.67±2.92**
10	37.87±3.33	36.40±2.02	**54.13±2.87**
11	34.40±4.41	37.07±3.13	**38.93±5.02**

Inter-brain coupling and decoding analysis using intra and inter frequency bands in motor imagery

To further investigate the frequency characteristics of collaborative neural patterns, we conducted a comparative analysis of different combinations of intra-frequency and cross-frequency. The decoding performance under different frequency configurations is shown in Table 1. The results indicate that in the vast majority of participant pairs, the β band exhibits the highest classification accuracy, highlighting its central role in representing motor imagery intentions. The α band and its cross-frequency interaction with the β band also demonstrate certain classification performance.

Table 2: Decoding accuracy across varying segment lengths (1s, 2s, 4s). Bold numbers denote the highest accuracy achieved for each group.

Group	1s	2s	4s
1	58.95±1.04	66.67±1.09	**72.87±2.60**
2	47.68±1.00	47.30±1.28	**55.73±0.86**
3	**37.72±0.32**	36.13±1.02	35.67±2.65
4	**34.62±0.36**	32.93±0.38	32.27±1.42
5	72.40±0.19	79.17±0.40	**86.27±0.55**
6	45.78±0.25	49.03±0.77	**49.33±0.84**
7	**38.88±0.68**	38.03±1.06	34.87±1.34
8	**42.65±5.33**	36.93±3.22	39.40±3.90
9	42.05±0.36	42.43±1.35	**42.47±2.71**
10	48.98±0.99	50.27±1.28	**51.40±1.58**
11	37.55±1.07	**38.87±1.65**	35.67±1.68

Interestingly, the hyperconnectivity preservation results shown in Figure 4 reveal a unique pattern: the highest number of significant interbrain functional connections is observed at the intersection (cross-frequency) of α and β bands. Although β oscillations are closely related to local motor execution and imagination, $(\alpha - \beta)$ cross-frequency coupling appears to serve as the main bridge for interbrain synchronization during common tasks. This difference suggests that, while local decoding heavily relies on β rhythms, the coordination between participants is more robustly manifested through cross-frequency spectral interactions between α and

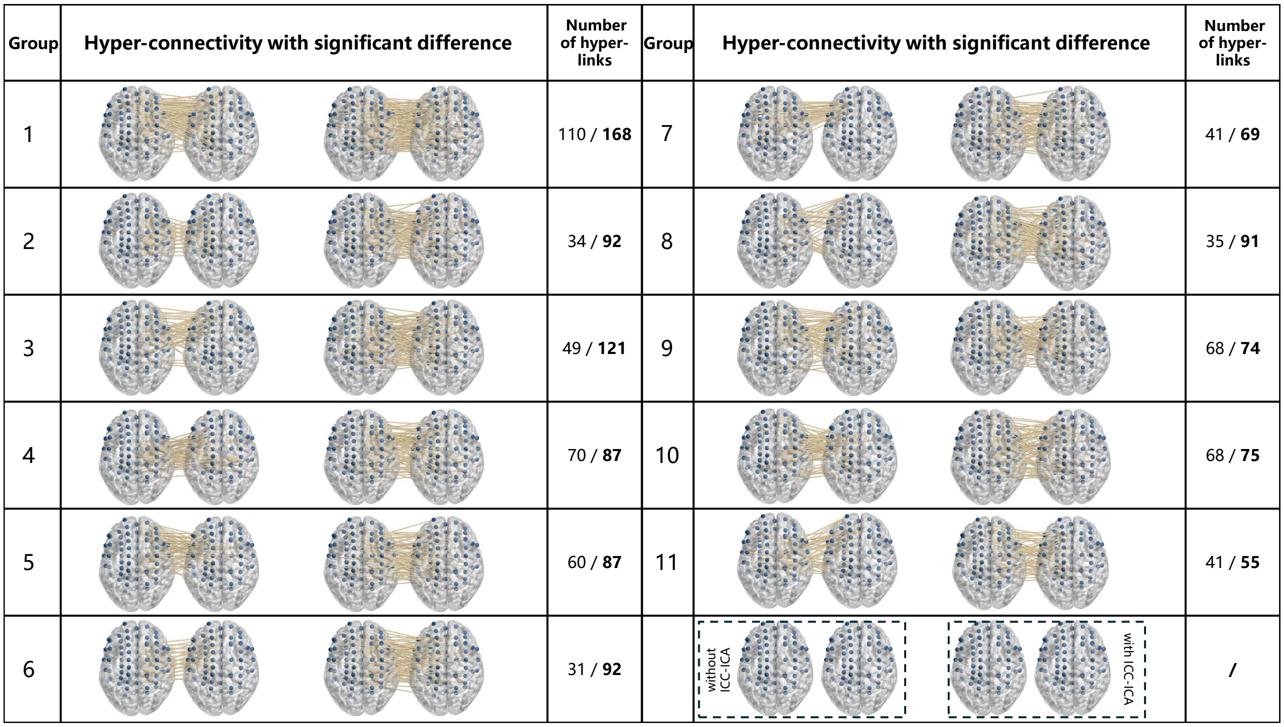

Figure 5: Visualization of significant inter-brain hyperconnectivity across groups. The comparison reveals the difference between the baseline (left) and the proposed ICC-ICA (right). The numerical column indicates the count of links, highlighting that ICC-ICA explicitly preserves critical synchronous neural oscillations in motor-related areas.

β oscillations, which are effectively restored by our ICC-ICA algorithm.

Inter-brain coupling and decoding analysis using different temporal segmentation in motor imagery

We further evaluated the influence of window duration (1s, 2s, 4s) on decoding accuracy and coupling stability. As shown in Table 2, decoding performance positively correlated with window length, with 4s segments achieving the highest accuracy, suggesting that longer integration enhances oscillatory feature discrimination.

Conversely, hyper-connectivity analysis (Figure 6) revealed an inverse trend: shorter segments (1s) yielded the highest number of significant links but exhibited larger standard deviations. This indicates that while brief windows capture transient synchronization, they are prone to statistical noise and spurious correlations. Longer segments provide a more conservative but robust estimation of inter-brain coupling. These findings highlight a critical trade-off between sensitivity to dynamic fluctuations and the statistical reliability of neural markers.

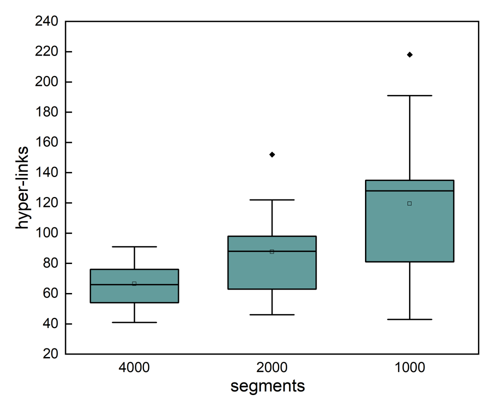

Figure 6: Distribution of hyper-links detected under varying segment lengths.

Conclusion

We propose ICC-ICA, a framework integrating coupled gradients to resolve the trade-off between artifact removal and inter-brain dependency preservation. The method outperforms standard ICA and CSP/LDA benchmarks, improving decoding accuracy by 0.8% and 1.76%, respectively, while significantly enhancing the detection of PLV-based motor connectivity. Neurophysiological analyses reveal that while β rhythms dominate local decoding, $(\alpha - \beta)$ cross-frequency coupling drives social coordination. The ICC-ICA provides a robust foundation for advancing collaborative BCI and hyperscanning research.

Acknowledgments

This work was supported by National Science Foundation of China under Grant No. 62301196; Zhejiang Provincial Natural Science Foundation of China under Grant No. LQ24F020035; the "Pioneer" and "Leading Goose" R&D Program of Zhejiang under Grant No. 2025C04001 and No. 2023C03026 and was also supported by Laboratory of Brain Machine Collaborative Intelligence of Zhejiang Province under Grant No. 2020E10010. It was also supported by the Central Government-Guided Local Science and Technology Development Fund (Grant No. 2025ZY01045) and the Zhejiang Provincial Key Laboratory of Brain Computer Collaborative Intelligence Technology and Applications (Grant No.2025E10015). Corresponding auhtor: Li Zhu.

References

Almutairi, H., Hassan, G. M., & Datta, A. (2023). Classification of sleep stages from eeg, eog and emg signals by ssnet. *arXiv preprint arXiv:2307.05373*.

Apicella, A., Arpaia, P., Frosolone, M., Improta, G., Moccaldi, N., & Pollastro, A. (2022). Eeg-based measurement system for monitoring student engagement in learning 4.0. *Scientific Reports*, *12*(1), 5857.

Bardel, B., Chalah, M. A., Bensais-Rueda, R., Créange, A., Lefaucheur, J.-P., & Ayache, S. S. (2024). Event-related desynchronization and synchronization in multiple sclerosis. *Multiple sclerosis and related disorders*, *86*, 105601.

Buchholz, S., Besserve, M., & Schölkopf, B. (2022). Function classes for identifiable nonlinear independent component analysis. *Advances in Neural Information Processing Systems*, *35*, 16946–16961.

Byrne, A., Hewitt, D., Henderson, J., Newton-Fenner, A., Roberts, H., Tyson-Carr, J., Giesbrecht, T., & Stancak, A. (2025). Changes in anticipatory event-related desynchronization (erd) during an effortful task when incentivized with a gain or loss. *Journal of Neuroscience, Psychology, and Economics*, *18*(3), 75.

Carollo, A., & Esposito, G. (2024). Hyperscanning literature after two decades of neuroscientific research: A scientometric review. *Neuroscience*, *551*, 345–354.

Cherloo, M. N., Amiri, H. K., & Daliri, M. R. (2022). Spatio-spectral cca (ss-cca): A novel approach for frequency recognition in ssvep-based bci. *Journal of Neuroscience Methods*, *371*, 109499.

Czeszumski, A., Eustergerling, S., Lang, A., Menrath, D., Gerstenberger, M., Schuberth, S., Schreiber, F., Rendon, Z. Z., & König, P. (2020). Hyperscanning: A valid method to study neural inter-brain underpinnings of social interaction. *Frontiers in Human Neuroscience*, *14*, 39.

Gao, L., Li, D., Liu, X., & Liu, G. (2022). Enhanced chiller faults detection and isolation method based on independent component analysis and k-nearest neighbors classifier. *Building and Environment*, *216*, 109010.

Hyvärinen, A., & Oja, E. (2000). Independent component analysis: Algorithms and applications. *Neural networks*, *13*(4-5), 411–430.

Lin, J., Qiu, S., Tan, X., & Zhuang, Y. (2023). Measuring the relationship between morphological spatial pattern of green space and urban heat island using machine learning methods. *Building and Environment*, *228*, 109910.

Liu, Z., Shore, J., Wang, M., Yuan, F., Buss, A., & Zhao, X. (2021). A systematic review on hybrid eeg/fnirs in brain-computer interface. *Biomedical Signal Processing and Control*, *68*, 102595.

Marques, L. M., Barbosa, S. P., Pacheco-Barrios, K., Goncalves, F. T., Imamura, M., Battistella, L. R., Simis, M., & Fregni, F. (2022). Motor event-related synchronization as an inhibitory biomarker of pain severity, sensitivity, and chronicity in patients with knee osteoarthritis. *Neurophysiologie Clinique*, *52*(6), 413–426.

Pronina, M. V., Ponomarev, V. A., Poliakov, Y. I., Martins-Mourao, A., Plotnikova, I. V., Müller, A., & Kropotov, Y. D. (2023). Event-related eeg synchronization and desynchronization in patients with obsessive–compulsive disorder. *Psychophysiology*, *60*(12), e14403.

Salvatore, C., Valeriani, D., Piccialli, V., & Bianchi, L. (2022). Optimized collaborative brain-computer interfaces for enhancing face recognition. *IEEE Transactions on Neural Systems and Rehabilitation Engineering*, *30*, 1223–1232.

Sharma, M., Yadav, A., Tiwari, J., Karabatak, M., Yildirim, O., & Acharya, U. R. (2022). An automated wavelet-based sleep scoring model using eeg, emg, and eog signals with more than 8000 subjects. *International Journal of Environmental Research and Public Health*, *19*(12), 7176.

Speer, S. P., Mwilambwe-Tshilobo, L., Tsoi, L., Burns, S. M., Falk, E. B., & Tamir, D. I. (2024). Hyperscanning shows friends explore and strangers converge in conversation. *Nature communications*, *15*(1), 7781.

Yan, R., Shang, Z., Xu, H., Wen, J., Zhao, Z., Chen, X., & Gao, R. X. (2023). Wavelet transform for rotary machine fault diagnosis: 10 years revisited. *Mechanical systems and signal processing*, *200*, 110545.

Yao, Y., Zhang, Z.-y., & Zhao, Y. (2023). Stock index forecasting based on multivariate empirical mode decomposition and temporal convolutional networks. *Applied Soft Computing*, *142*, 110356.

Zhao, S., Zhang, B., Yang, J., Zhou, J., & Xu, Y. (2024). Linear discriminant analysis. *Nature Reviews Methods Primers*, *4*(1), 70.